

FADDEEV CALCULATION FOR ELASTIC NUCLEON-DEUTERON  
SCATTERING AT 3 MeV LAB ENERGY

V. M. SUSLOV<sup>a</sup>, I. FILIKHIN<sup>a</sup>, B. VLAHOVIĆ<sup>a</sup>, M. A. BRAUN<sup>b</sup> and I. ŠLAUS<sup>c</sup>

<sup>a</sup>*Physics Department, North Carolina Central University, 1801 Fayetteville Street,  
Durham, NC 27707, U. S. A.*

<sup>b</sup>*Department of Theoretical Physics, Saint-Petersburg State University,  
198504, Ul'yanovskaya 1, Petrodvorets, Saint-Petersburg, Russia*

<sup>c</sup>*R. Bošković Institute, 10000 Zagreb, Croatia*

Received 12 July 2011; Accepted 16 November 2011  
Online 9 February 2012

A new computational method for solving the nucleon-deuteron breakup scattering problem has been applied to study the elastic neutron- and proton-deuteron scattering on the basis of the configuration-space Faddeev-Noyes-Noble-Mercuriev equations. This method is based on the spline-decomposition in the angular variable and on a generalization of the Numerov method for the hyperradius. The Mercuriev-Gignoux-Laverne approach has been generalized for arbitrary nucleon-nucleon potentials and with an arbitrary number of partial waves. The nucleon-deuteron observables at the incident nucleon energy 3 MeV have been calculated using the charge-independent AV14 nucleon-nucleon potential including the Coulomb force for the proton-deuteron scattering. Results have been compared with those of other authors and with experimental proton-deuteron scattering data.

PACS numbers: 21.45.+v, 11.80.Jy, 25.45.De

UDC 539.128, 539.172

Keywords: nucleon-deuteron breakup, proton-deuteron scattering, Faddeev equations, incident nucleon energy 3 MeV, AV14 nucleon-nucleon potential

## 1. Introduction

There is an impressive amount of nucleon-deuteron scattering data: proton-deuteron and neutron-deuteron elastic and breakup data: total, partial and differential cross sections and spin observables involving nucleon and deuteron beams. The data are compared with the rigorous three-body theory: Faddeev-equations-based theory using as input realistic high-precision nucleon-nucleon potentials, and includ-

ing model three-nucleon forces [1]. In some calculations Coulomb force has been included [2]. Nucleon-nucleon (NN) potentials used in rigorous three-nucleon (3N) calculations describe the NN database with  $\chi^2/\text{degree of freedom}$  approximately equal to one. These are AV18 [3], CD-Bonn [4] and several Nijmegen potentials [5] and to a lesser degree AV14 [6]. Among three nucleon forces (3NF) are Tucson-Melbourne and its various modifications [7], and Urbana potentials [8]. Based on the chiral effective field theory (EFT), NN and 3N potentials have been developed [9] and they have been used in a rigorous 3N calculations [10]. A local version of the effective field theory at next-to-next to leading order labeled N<sup>2</sup>LO is given in Ref. [11].

In spite of this enormous progress in the three-nucleon studies, there are several important cases where the rigorous three-nucleon calculations have failed to explain the data [12] and these discrepancies are established with very high precision. Among the most important discrepancies are the  $A_y$  puzzle in nucleon-deuteron (Nd) elastic scattering [13], the star configuration in the Nd breakup reaction [14], quasi-free scattering (QFS) cross section [1] and the nd backward angle scattering at energies between 50 and 100 MeV [15]. Some three-nucleon data show clear evidence for the 3NF, but some are in better agreement with the calculation if the 3NF are not included. High-precision realistic potentials (Nijmegen, Bonn, Paris, Urbana) are not phase equivalent and they predict different triton binding energies, they have different short-range potentials and some differ conceptually. It is hoped that EFT will give an answer, but it is still unclear.

There are more 3N data involving charged particles and therefore, calculations rigorously including electromagnetic interactions are of paramount importance. The pd scattering has been studied by using hyperspherical harmonic method and Kohn variational principle [16] and by using the screening and renormalization procedure [17]. At 3 MeV, calculations have been done using high precision realistic potentials and 3NF [18], while at energies above the threshold for the deuteron breakup, only calculations using screening and renormalization have been done. The screening method cannot be applied to energies below 1 MeV and this is a serious limitation.

In this article we present the development of an alternative method for studying the proton-deuteron (pd) system based on the direct numerical solution of the Faddeev-Noyes-Noble-Merkuriev (FNNM) equations in configuration space. This approach was initiated by Merkuriev et al. (MGL) [19] who derived general formulae for nd breakup scattering. This method has been originally applied to study nd and pd elastic and breakup scattering but limited only to nuclear S-waves interaction and to simple NN potentials [20]. In the present work we generalize the MGL approach to any high precision realistic potential for both nd and pd for elastic processes.

This paper is organized as follows: in Section 2 we describe a calculation in configuration space starting with the general formalism in Subsection 2.1, followed by Numerov method in Subsection 2.2. Our novel method for solution is given in Subsection 2.3. Our results are presented in Section 3. Comparisons of our results with the previous calculations and with the data are discussed in Section 4. Finally, our summary and conclusion are given in Section 5.

## 2. Three-nucleon Faddeev calculation in configuration space - our new computational method

### 2.1. Formalism

The starting point for studying interactions between nucleons in three-body systems is the solution of the Schrödinger equation  $H\Psi = E\Psi$  for nuclear Hamiltonian such as

$$H = -\frac{\hbar^2}{2m} \sum_{i=1}^3 \nabla_i^2 + V_c + \sum_{j<k} V_{jk} \left( + \sum_{j<k<l} V_{jkl} \right), \quad (1)$$

where  $V_c$  and  $V_{jk}$  are the Coulomb and nuclear potentials, respectively. In this study we neglected three-nucleon forces  $V_{jkl}$ .

Writing the total wave function as

$$\Psi = \Phi_1 + \Phi_2 + \Phi_3 = (1 + P^+ + P^-)\Phi_1, \quad (2)$$

the Schrödinger equation for three identical particles can be reduced into a single Faddeev equation, which in Jacobi's vectors  $\vec{x}_1, \vec{y}_1$  has the form

$$\left[ -\frac{\hbar^2}{m} (\Delta_{\vec{x}_1} + \Delta_{\vec{y}_1}) + V_c + V(\vec{x}_1) - E \right] \Phi(\vec{x}_1, \vec{y}_1) = -V(\vec{x}_1)(P^+ + P^-)\Phi(\vec{x}_1, \vec{y}_1), \quad (3)$$

where the operators  $P^\pm$  are the cyclic permutation operators for the three particles which interchange any pair of nucleons ( $P^+ : 123 \rightarrow 231, P^- : 123 \rightarrow 312$ ). The Coulomb potential has the following form

$$V_c = \sum_{\alpha} \frac{n}{|x_{\alpha}|} \prod_{i \in \alpha} \frac{1}{2} (1 + \tau_z^i), \quad n = \frac{me^2}{\hbar^2}, \quad (4)$$

where  $e^2 = 1.44 \text{ MeV fm}$  and  $\hbar^2/m = 41.47 \text{ MeV fm}^2$ . The sum runs over  $\alpha = 1, 2, 3$  for the three possible pairs and the product of the isospin projection operators runs over the indices  $i$  of the particles belonging to the pair  $\alpha$ . As independent coordinates, we take the Jacobi vectors  $\vec{x}_{\alpha}, \vec{y}_{\alpha}$ . For the pair  $\alpha=1$ , they are related to particle coordinates by the formulae

$$\vec{x}_1 = \vec{r}_2 - \vec{r}_3, \quad \vec{y}_1 = \frac{\vec{r}_2 + \vec{r}_3}{2} - \vec{r}_1, \quad (5)$$

for  $\alpha = 2, 3$  one has to make cyclic permutations of the indices in Eq. (5). The Jacobi vectors with different  $\alpha$ 's are linearly related by the orthogonal transformation

$$\begin{pmatrix} \vec{x}_{\alpha} \\ \vec{y}_{\alpha} \end{pmatrix} = \begin{pmatrix} C_{\alpha\beta} & S_{\alpha\beta} \\ -S_{\alpha\beta} & C_{\alpha\beta} \end{pmatrix} \begin{pmatrix} \vec{x}_{\beta} \\ \vec{y}_{\beta} \end{pmatrix}, \quad C_{\alpha\beta}^2 + S_{\alpha\beta}^2 = 1, \quad (6)$$

where

$$C_{\alpha\beta} = -\sqrt{\frac{m_\alpha m_\beta}{(M - m_\alpha)(M - m_\beta)}}, \quad S_{\alpha\beta} = (-)^{\beta-\alpha} \text{sgn}(\beta - \alpha) \sqrt{1 - C_{\alpha\beta}^2}, \quad (7)$$

$$M = \sum_{\alpha=1}^3 m_\alpha.$$

To perform numerical calculations for arbitrary nuclear potential, we use MGL approach [19]. For  $pd$  scattering, the FNNM equations for partial components can be written in the following form (here we omit the index 1)

$$\left[ E + \frac{\hbar^2}{m} (\partial_x^2 + \partial_y^2) - v_\alpha^\lambda(x, y) \right] \Phi_\alpha^{\lambda_0, s_0, M_0}(x, y) = \sum_\beta \left[ v_{1, \alpha\beta} + \sum_\tau (v_\tau^+ c_{\tau, \alpha\beta}^{M_0^+} + v_\tau^- c_{\tau, \alpha\beta}^{M_0^-}) \right]$$

$$\times \Phi_\beta^{\lambda_0, s_0, M_0}(x, y) + \sum_\beta v_{\alpha\beta}(x) \left[ \Phi_\beta^{\lambda_0, s_0, M_0}(x, y) + \int_{-1}^1 du \sum_\gamma g_{\beta\gamma}(y/x, u) \Phi_\gamma^{\lambda_0, s_0, M_0}(x', y') \right]. \quad (8)$$

Here Greek subindexes denote state quantum numbers:  $\alpha = \{l, \sigma, j, s, \lambda, t, T\}$ , where  $l, \sigma, j$  and  $t$  are the orbital, spin, total angular momenta and isospin of a pair of nucleons,  $\lambda$  is the orbital momentum of the third nucleon relative to the c.m.s. of a pair nucleons, and  $s$  is the total "spin" ( $\mathbf{s} = \mathbf{1}/2 + \mathbf{j}$ ).  $\mathbf{M} = \vec{\lambda} + \vec{s}$  is the total three-particle angular momentum, and the value of total isospin is  $T$ . In Eqs. (8),  $v_1$  and coefficients  $c^{M_0^\pm}$  depending on quantum state numbers of channel combined with  $v^\pm$  are matrix elements of the Coulomb potential projected onto the MGL basis. For given  $\alpha$  and  $\beta$ , summation over  $\tau$  in Eqs. (8) is finite. If  $\alpha = \{l\sigma js\lambda tT\}$  and  $\beta = \{l'\sigma' j's'\lambda't'T'\}$  then values of  $\tau$  are restricted by the following inequality,

$$\max(|l - l'|, |\lambda - \lambda'|) \leq \tau \leq \min(l + l', \lambda + \lambda').$$

This means that for a chosen set of basic states, Eqs. (8) take into account the Coulomb interaction exactly (although the latter has been expanded in partial waves).

The geometrical function  $g_{\beta\gamma}(x, y, u)$  is the representative of the permutation operator  $P^+ + P^-$  in MGL basis [19]

$$g_{\alpha'\alpha}(y/x, u) = g_{\alpha'\alpha}(\theta, u) = g_{\alpha'\alpha}(\theta, \theta')$$

$$= (-1)^{\lambda+\lambda'+J+J'} [(2J+1)(2J'+1)(2s+1)(2s'+1)]^{1/2} \sum_{LS} (2S+1)(2L+1)$$

$$\left\{ \begin{matrix} l & \sigma & J \\ 1/2 & s & S \end{matrix} \right\} \left\{ \begin{matrix} l' & \sigma' & J' \\ 1/2 & s' & S \end{matrix} \right\} \left\{ \begin{matrix} \lambda & l & L \\ S & M & s \end{matrix} \right\} \left\{ \begin{matrix} \lambda' & l' & L \\ S & M & s' \end{matrix} \right\}$$

$$\langle \chi_{1/2\sigma'}^S \eta_{1/2,t'}^T | P^+ | \chi_{1/2\sigma}^S \eta_{1/2,t}^T \rangle h_{\lambda'l\lambda}^L(y/x, u). \quad (9)$$

Function  $h$  is the representative of the permutation operator  $P^+ + P^-$  in the  $\lambda + l = L$  basis

$$\begin{aligned}
 h_{\lambda'l'\lambda l}^L(y/x, u) &= h_{\lambda'l'\lambda l}^L(\theta, u) = h_{\lambda'l'\lambda l}^L(\theta, \theta') \\
 &= \frac{xy}{x'y'} (-1)^{l+L} \frac{(2\lambda + 1)(2l + 1)}{2^{\lambda+l}} [(2\lambda)!(2l)!(2\lambda' + 1)(2l' + 1)]^{1/2} \\
 &\quad \sum_{k=0} (-1)^k (2k + 1) P_k(u) \sum_{\lambda_1 + \lambda_2 = \lambda, l_1 + l_2 = l} \frac{y^{\lambda_1 + l_1} x^{\lambda_2 + l_2}}{y'^{\lambda} x'^l} (-1)^{l_2} \\
 &\quad \frac{(\sqrt{3})^{\lambda_2 + l_1}}{[(2\lambda_1)!(2\lambda_2)!(2l_1)!(2l_2)!]^{1/2}} \sum_{\lambda'' l''} (2\lambda'' + 1)(2l'' + 1) \\
 &\quad \begin{pmatrix} \lambda_1 & l_1 & \lambda'' \\ 0 & 0 & 0 \end{pmatrix} \begin{pmatrix} \lambda_2 & l_2 & l'' \\ 0 & 0 & 0 \end{pmatrix} \begin{pmatrix} k & \lambda'' & \lambda' \\ 0 & 0 & 0 \end{pmatrix} \begin{pmatrix} k & l'' & l' \\ 0 & 0 & 0 \end{pmatrix} \\
 &\quad \left\{ \begin{matrix} l' & \lambda' & L \\ \lambda'' & l'' & k \end{matrix} \right\} \left\{ \begin{matrix} \lambda_1 & \lambda_2 & \lambda \\ l_1 & l_2 & l \\ \lambda'' & l'' & L \end{matrix} \right\}. \tag{10}
 \end{aligned}$$

The index  $k$  runs from zero to  $(\lambda' + l' + \lambda + l)/2$ . The (...) are the  $3j$  symbols,

$$\begin{pmatrix} j_1 & j_2 & j_3 \\ m_1 & m_2 & m_3 \end{pmatrix} = (-1)^{j_3 + m_3 + 2j_1} \frac{1}{\sqrt{2j_3 + 1}} C_{j_1 - m_1 j_2 - m_2}^{j_3 m_3}.$$

The centrifugal potential is

$$v_{\alpha}^{\lambda l} = \frac{\hbar^2}{m} \left[ \frac{l(l + 1)}{x^2} + \frac{\lambda(\lambda + 1)}{y^2} \right], \tag{11}$$

and nucleon-nucleon potentials are  $v_{\alpha\alpha'}(x) = \langle \alpha | v(\mathbf{x}) | \alpha' \rangle = \delta_{\lambda\lambda'} \delta_{ss'} \delta_{\sigma\sigma'} \delta_{JJ'} v_{ll'}^{\sigma J}$ , where  $v_{ll'}^{\sigma J}$  are the potential representatives in the two-body basis  $\mathcal{Y}_{l\sigma}^{JJ_z}(\mathbf{\bar{x}})$  (most often abbreviated as  ${}^{2\sigma+1}l_J$ ).

The set of partial differential equation Eqs. (8) must be solved for functions satisfying the regularity conditions

$$\Phi_{\alpha}^{\lambda_0 s_0 M_0}(0, \theta) = \Phi_{\alpha}^{\lambda_0 s_0 M_0}(\rho, 0) = \Phi_{\alpha}^{\lambda_0 s_0 M_0}(\rho, \pi/2) = 0. \tag{12}$$

The asymptotic conditions for pd elastic scattering have the following form [21]

$$\begin{aligned}
 \Phi_{1, \bar{\alpha}}^{\lambda_0 s_0 M_0}(x, y) &\sim \left\{ \delta_{\lambda\lambda_0} \delta_{ss_0} \delta_{\sigma_1} \delta_{j_1} e^{i\Delta_{\lambda}^c} F_{\lambda}^c(qy) + \right. \\
 &e^{-i\Delta_{\lambda}^c} \left( G_{\lambda}^c(qy) + iF_{\lambda}^c(qy) \right) a_{\lambda s \lambda_0 s_0}^{M_0} \left. \right\} \psi_l(x), \\
 &x \text{ finite, } y \rightarrow \infty,
 \end{aligned} \tag{13}$$

where  $\Delta_\lambda^c = \arg \Gamma(\lambda + 1 + i\nu)$  is the Coulomb phase and  $\nu$  is equal  $n/(\sqrt{3}q)$ ,  $\psi_l$  is  $l$ -th component of deuteron wave function ( $l = 0, 2$ ), and  $F^c$  and  $G^c$  are the regular and irregular Coulomb functions, respectively.

The S-matrix is defined as follows

$$S_{\lambda s \lambda_0 s_0}^{M_0} = \delta_{\lambda \lambda_0} \delta_{s s_0} \delta_{\sigma 1} \delta_{j 1} e^{i2\Delta_\lambda^c} + 2i a_{\lambda s \lambda_0 s_0}^{M_0}. \tag{14}$$

At energies below threshold, the S-matrix is unitary and may be presented as

$$S = e^{2i\Delta},$$

where  $\Delta$  is the Hermitean matrix of scattering phases. From (13) we then find that the matrix of partial elastic amplitudes  $a$  has the structure

$$a = \frac{(e^{2i\Delta} - e^{2i\Delta^c})}{2i} = \frac{e^{2i\Delta^c} (e^{2i\delta} - 1)}{2i}, \tag{15}$$

where  $\Delta^c$  is a diagonal matrix of Coulomb phases and  $\Delta$  is the Hermitean matrix of scattering phases. The phases  $\delta = \Delta - \Delta^c$  are the contribution to the scattering phase due to the nuclear interaction.

To simplify the numerical solution of the FNNM equations, we write down Eqs. (8) in the polar coordinate system ( $\rho^2 = x^2 + y^2$  and  $\tan \theta = y/x$ )

$$\begin{aligned} & \left[ E + \frac{\hbar^2}{m} \left( \frac{\partial^2}{\partial \rho^2} + \frac{1}{\rho^2} \frac{\partial^2}{\partial \theta^2} + \frac{1}{4\rho^2} \right) - v_\alpha^\lambda(\rho, \theta) \right] U_{\alpha}^{\lambda_0 s_0 M_0}(\rho, \theta) = \frac{n}{\rho} \sum_{\beta} Q_{\alpha\beta} U_{\beta}^{\lambda_0 s_0 M_0}(\rho, \theta) \\ & + \sum_{\beta} v_{\alpha\beta}(\rho, \theta) \left[ U_{\beta}^{\lambda_0 s_0 M_0}(\rho, \theta) + \int_{-1}^1 du \sum_{\gamma} g_{\beta\gamma}(\theta, u, \theta'(\theta, u)) U_{\gamma}^{\lambda_0 s_0 M_0}(\rho, \theta') \right], \end{aligned} \tag{16}$$

where

$$\cos^2 \theta'(u, \theta) = \frac{1}{4} \cos^2 \theta - \frac{\sqrt{3}}{2} \cos \theta \sin \theta \cdot u + \frac{3}{4} \sin^2 \theta, \tag{17}$$

and the first derivative in the radius is eliminated by the substitution  $U = \rho^{-1/2} \Phi$ . In Eq. (16),  $Q_{\alpha\beta}$  is the overall matrix sum of the Coulomb potential.

In the case of neutron-deuteron elastic scattering, one has to set the “charge”  $n$  equal to zero. This leads to equality to zero of the Coulomb phases  $\Delta_\lambda^c$ , and the Coulomb functions  $F_\lambda^c$  and  $G_\lambda^c$  are reduced to the regularized spherical Bessel functions  $\hat{j}_\lambda$  and  $-\hat{y}_\lambda$ , respectively.

## 2.2. Numerov method

Modification of the Numerov method for the set of the differential equations (16) does not present any difficulties in principle. As is well known, the Numerov

method is an efficient algorithm for solving second-order differential equations. The important feature of the equations for the application of Numerov's method is that the first derivative has to be absent. The aim of this method is to improve the accuracy of the finite-difference approximation for the second derivative. Starting from the Taylor expansion truncated after the sixth derivative for two points adjacent to  $x_n$ , that is for  $x_{n-1}$  and  $x_{n+1}$  one sums these two expansions to give a new computational formula that includes the fourth derivative. This derivative can be found by straightforward differentiation of the second derivative from the initial second-order differential equation (see the details in Ref. [22]). For brevity, we omit the corresponding derivation and present only the final formula of Numerov's method for the FNNM equations (omitting the upper indices  $\lambda_0 s_0 M_0$ )

$$\begin{aligned}
 & - \left[ E + \frac{12}{(\Delta\rho)^2} + \left(1 + \frac{2\Delta\rho}{\rho_j}\right) \frac{T_\alpha(\theta)}{\rho_j^2} \right] U_\alpha(\rho_{j-1}, \theta) + n \sum_\beta \frac{Q_{\alpha\beta}(\theta)}{\rho_j} \left(1 + \frac{\Delta\rho}{\rho_j}\right) U_\beta(\rho_{j-1}, \theta) \\
 & + \sum_\beta (v_{\alpha\beta}(\rho_j, \theta) - \Delta\rho v'_{\alpha\beta}(\rho_j, \theta)) (U_\beta(\rho_{j-1}, \theta) + \sum_\gamma \int_{\theta^-}^{\theta^+} d\theta' g_{\beta\gamma}(\theta, \theta') U_\gamma(\rho_{j-1}, \theta')) \\
 & - 2 \left[ 5E - \frac{12}{(\Delta\rho)^2} + \left(5 + \frac{3\Delta\rho}{\rho_j}\right) \frac{T_\alpha(\theta)}{\rho_j^2} \right] U_\alpha(\rho_j, \theta) + 2n \sum_\beta \frac{Q_{\alpha\beta}(\theta)}{\rho_j} \left(5 + \frac{(\Delta\rho)^2}{\rho_j^2}\right) U_\beta(\rho_j, \theta) \\
 & + \sum_\beta (10v_{\alpha\beta}(\rho_j, \theta) + (\Delta\rho)^2 v''_{\alpha\beta}(\rho_j, \theta)) (U_\beta(\rho_j, \theta) + \sum_\gamma \int_{\theta^-}^{\theta^+} d\theta' g_{\beta\gamma}(\theta, \theta') U_\gamma(\rho_j, \theta')) \\
 & - \left[ E + \frac{12}{(\Delta\rho)^2} + \left(1 - \frac{2\Delta\rho}{\rho_j}\right) \frac{T_\alpha(\theta)}{\rho_j^2} \right] U_\alpha(\rho_{j+1}, \theta) + n \sum_\beta \frac{Q_{\alpha\beta}(\theta)}{\rho_j} \left(1 - \frac{\Delta\rho}{\rho_j}\right) U_\beta(\rho_{j+1}, \theta) \\
 & + \sum_\beta (v_{\alpha\beta}(\rho_j, \theta) + \Delta\rho v'_{\alpha\beta}(\rho_j, \theta)) (U_\beta(\rho_{j+1}, \theta) + \sum_\gamma \int_{\theta^-}^{\theta^+} d\theta' g_{\beta\gamma}(\theta, \theta') U_\gamma(\rho_{j+1}, \theta')) = 0,
 \end{aligned} \tag{18}$$

where

$$T_\alpha(\theta) = \frac{\partial^2}{\partial\theta^2} - \frac{l(l+1)}{\cos^2\theta} - \frac{\lambda(\lambda+1)}{\sin^2\theta} + \frac{1}{4}.$$

In Eq. (18),  $\rho_j$  is the  $j$ -th current point for hyperradius  $\rho \in (0, R_{\max})$  in the radial grid ( $j = 1, 2, \dots, N_\rho$ ),  $\Delta\rho_j$  is the radial step-interval.

To ensure the accuracy of order  $(\Delta\theta)^4$  for the approximation in the angular variable, Hermitian splines of the fifth degree have been used (see Ref. [23]). These splines are local and each spline  $S_{\sigma i}(x)$  is defined for  $x$  belonging to two adjacent subintervals  $[x_{i-1}, x_i]$  and  $[x_i, x_{i+1}]$ . Their analytical form is fixed by the following smoothness conditions

$$S_{\sigma i}(x_{i-1}) = 0, \quad S_{\sigma i}(x_{i+1}) = 0, \quad \sigma = 0, 1, 2, \tag{19}$$

and

$$\begin{aligned} S_{0i}(x_i) &= 1, & S'_{0i}(x_i) &= 0, & S''_{0i}(x_i) &= 0, \\ S_{1i}(x_i) &= 0, & S'_{1i}(x_i) &= 1, & S''_{1i}(x_i) &= 0, \\ S_{2i}(x_i) &= 0, & S'_{2i}(x_i) &= 0, & S''_{2i}(x_i) &= 1. \end{aligned} \quad (20)$$

Expansion of the Faddeev component into basis of the Hermitian splines has the following form

$$U_\alpha(\rho, \theta) = \sum_{\sigma=0}^2 \sum_{j=0}^{N_\theta+1} S_{\sigma j}(\theta) C_{\alpha j}^\sigma(\rho), \quad (21)$$

where  $N_\theta + 1$  is the number of internal subintervals for the angular variable  $\theta \in [0, \pi/2]$ .

To reduce the resulting equation (18) to an algebraic problem, one should explicitly calculate the derivatives of NN potentials  $v_{\alpha\beta}(\rho, \theta)$  with respect to  $\rho$  and the second derivatives of splines  $S_{\sigma j}(\theta)$  with respect to  $\theta$ . It is convenient to express the second derivative of component  $U_\alpha$  with respect to  $\theta$  through  $U_\alpha$  itself using Eq. (21). Upon substituting the spline expansion (21) and expression for its second derivative into Eqs. (18), we use a collocation procedure with three Gaussian quadrature points per subinterval. As the number of internal breakpoints for angular variable  $\theta$  is equal to  $N_\theta$ , the basis of quintic splines consists of  $3N_\theta + 6$  functions. Three of them should be excluded using the last two regularity conditions from (12) and continuity of the first derivative in  $\theta$  of the Faddeev component at either  $\theta = 0$  or  $\theta = \pi/2$ , as the collocation procedure yields  $3N_\theta + 3$  equations. Finally Eqs. (18) for the Faddeev components are to be written as the following matrix equation

$$\begin{aligned} A_1 U_1 + G_1 U_2 &= 0, \\ B_j U_{j-1} + A_j U_j + G_j U_{j+1} &= 0, & j &= 2, \dots, N_\rho - 1, \\ B_{N_\rho} U_{N_\rho-1} + A_{N_\rho} U_{N_\rho} &= -G_{N_\rho} U_{N_\rho+1}. \end{aligned} \quad (22)$$

In this equation, vector  $U_k = U(\rho_k)$  has dimension  $N_{\text{in}}$  and matrices  $A, B, G$ , derived from Eq. (18), have dimension  $N_{\text{in}} \times N_{\text{in}}$  where  $N_{\text{in}} = N_\alpha \times N_c$ , and  $N_\alpha$  is the number of partial waves and  $N_c = 3N_\theta + 3$  is the number of collocation points in the angular variable  $\theta$ .

### 2.3. The novel method of solution

To derive equations for calculation of elastic Nd amplitudes, the method of partial inversion [22] has been applied. We write down Eq. (22) in a matrix form

$$(D * U)_i = -\delta_{iN_\rho} G_{N_\rho} U_{N_\rho+1}. \quad (23)$$

Here the matrix  $D$  is of dimension  $N_\rho N_{\text{in}} \times N_\rho N_{\text{in}}$ , and  $N_\rho$  is the number of breakpoints in the hyperradius  $\rho$ . The form of this equation results from keeping the incoming wave in the asymptotic condition (13). As a consequence, the right hand



part of Eq. (23) has a single nonzero term marked with index  $N_\rho + 1$ . Sparse (tri-block-diagonal) structure of matrix  $D$  optimizes considerably the inversion problem.

Hyperradius  $\rho_{N_\rho+1} = R_{\max}$ , where  $R_{\max}$  is the cutoff radius at which the asymptotic condition Eq. (13) is implemented. By formal inversion of the matrix  $D$  in Eq. (23), the solution of the problem may be written in the following form

$$U_j = -D_{jN_\rho}^{-1} G_{N_\rho} U_{N_\rho+1}, \quad j = 1, 2, \dots, N_\rho. \quad (24)$$

In Eqs. (24) one should consider the last component of vector  $U$

$$U_{N_\rho} = -D_{N_\rho N_\rho}^{-1} G_{N_\rho} U_{N_\rho+1}. \quad (25)$$

Provided  $R_{\max}$  is large enough, the vector  $U_{N_\rho}$  on the left side of Eq. (25) may be replaced by the corresponding vector obtained by evaluating Eq. (13) at the radius  $\rho = \rho_{N_\rho}$ . As a result in the case  $M \geq 3/2$  we obtain three linear equations for the unknown amplitudes  $a_{\lambda s \lambda_0 s_0}^{M_0}$

$$\sum_{i=1}^3 a_{ij}^{M_0} \cdot \mathbf{v}^i = \mathbf{F}^j, \quad j = 1, 2, 3. \quad (26)$$

For  $M_0 = 1/2$ , the indices run over  $i, j = 1, 2$ . In these equations, indices  $i, j$  number the asymptotic values of pairs  $(\lambda s)$ , and vectors  $\mathbf{v}, \mathbf{F}$  are known quantities. For the sake of brevity, we do not display here their explicit form. As  $R_{\max} \rightarrow \infty$ , the set of Eqs. (26) has a set of constants  $a_{ij}^{M_0}$  as a solution. At finite  $R_{\max}$ , its solution is a vector  $a$  with generally different components corresponding to different angles.

For each value of  $j$ , linear equation (26) is overdetermined, since the number of equations is  $N_{in}$  and the number of unknowns is 3. Therefore it is natural to use the least-squares method (LSM) as was proposed in Ref. [22]. According to LSM, one has to minimize the following functional

$$\left\| \sum_{i=1}^3 a_{ij}^{M_0} \cdot \mathbf{v}^i - \mathbf{F}^j \right\|^2 = \min. \quad (27)$$

Differentiating this expression with respect to  $\text{Re} a_{ij}^{M_0}$  and  $\text{Im} a_{ij}^{M_0}$ , we obtain three(two) sets of linear complex equations of dimension  $3 \times 3$  ( $2 \times 2$  for  $M_0=1/2$ ), respectively.

$$\sum_{i=1}^3 a_{ij}^{M_0} \cdot (\mathbf{v}_k^*, \mathbf{v}^i) = (\mathbf{v}_k^*, \mathbf{F}^j), \quad j = 1, 2, 3, \quad k = 1, 2, 3, \quad (28)$$

where  $(\xi^*, f) = \sum_i \xi_i^* \cdot f_i$  is an ordinary scalar product. Now calculation of amplitudes  $a_{ij}^{M_0}$  is a trivial task.

### 2.4. Observables

To calculate observables for elastic scattering of nucleon from deuteron in the direction  $\hat{\mathbf{q}}'$  (initial direction  $\hat{\mathbf{q}}$  is along the  $z$ -axis), one has to derive the equation for the elastic amplitude as a function of scattering angle. Omitting this derivation, we represent the final expression for this amplitude in MGL basis

$$\hat{a}_{\sigma'_z, J'_z, \sigma_z, J_z}(\hat{\mathbf{q}}') = \sum_M \sum_{\lambda' s'} \sum_{\lambda s} i^{\lambda-\lambda'} \sqrt{\frac{2\lambda+1}{4\pi}} \quad (29)$$

$$C_{\lambda' M_z - \sigma'_z - J'_z, s' \sigma'_z + J'_z}^{MM_z} C_{\lambda 0, s \sigma_z + J_z}^{MM_z} C_{1/2 \sigma'_z, 1 J'_z}^{s' \sigma'_z + J'_z} C_{1/2 \sigma, 1 J_z}^{s \sigma_z + J_z} Y_{\lambda' M_z - \sigma'_z - J'_z}(\hat{\mathbf{q}}') a_{\lambda' s' \lambda s}^M,$$

with  $M_z = \sigma_z + J_z$ .

In Eq. (29),  $\sigma' \sigma'_z(\sigma, \sigma_z)$  and  $J' J'_z(J J_z)$  are spin and its projection for incoming (scattered) nucleon, and the deuteron in the rest (scattered deuteron), respectively. Thus, the nuclear part of the elastic amplitude is a  $(2 \times 2) \otimes (3 \times 3)$  matrix in the spin states of nucleon and deuteron, depending on the spherical angles  $\theta$  and  $\phi$ .

The situation is a little bit more complicated with the elastic scattering of proton from deuteron, since apart from the nuclear part, the elastic amplitude also contains the pure Coulomb part. Thus in the matrix notation, the resulting amplitude is a sum of two amplitudes

$$\hat{a}^{\text{tot}} = \hat{a} + \hat{a}^c, \quad (30)$$

where  $\hat{a}$  is the nuclear part of the same form as for the nd case and  $\hat{a}^c$  is the Coulomb part which is a unit matrix in spin states (this term does not change spins and depends only on  $\theta$ )

$$\hat{a}^c_{\sigma'_z, J'_z, \sigma_z, J_z}(\hat{\mathbf{q}}') = a^c(\theta) \delta_{\sigma'_z \sigma_z} \delta_{J'_z J_z}. \quad (31)$$

The amplitude  $a^c$  is as follows

$$a^c(\theta) = -\frac{n}{8\pi q \sqrt{3} \sin^2(\theta/2)} \exp(-i\nu \ln \sin^2(\theta/2) + 2i\eta^c). \quad (32)$$

The parameter  $\nu$  is defined by the ratio  $\nu = 2n/(3q)$ ,  $q$  is the wave vector of a proton, the parameter  $n$  is given in Eq. (4), and  $\eta^c = \arg \Gamma(1 + i\nu)$ .

The spin observable formulas can be taken from the review [1]. They are expressed via spin  $2 \times 2$  matrices  $\sigma_i$  for the nucleon and  $3 \times 3$  matrices  $\mathcal{P}_i$  and  $\mathcal{P}_{ik}$  for the deuteron. The latter are related to the deuteron spin matrices  $S_i$

$$S_x = \frac{1}{\sqrt{2}} \begin{pmatrix} 0 & 1 & 0 \\ 1 & 0 & 1 \\ 0 & 1 & 0 \end{pmatrix}, \quad S_y = \frac{1}{\sqrt{2}} \begin{pmatrix} 0 & -i & 0 \\ i & 0 & -i \\ 0 & i & 0 \end{pmatrix}, \quad S_z = \begin{pmatrix} 1 & 0 & 0 \\ 0 & 0 & 0 \\ 0 & 0 & -1 \end{pmatrix}. \quad (33)$$

One has  $\mathcal{P}_i = S_i$ ,  $\mathcal{P}_{ik} = 3/2(S_i S_k + S_k S_i)$ ,  $\mathcal{P}_{zz} = 3S_z S_z - 2I$ , and  $\mathcal{P}_{xx} - \mathcal{P}_{yy} = 3(S_x S_x - S_y S_y)$ .

Nucleon analyzing powers  $A_k$  are

$$A_k = \frac{\text{Tr}(\widehat{a}\sigma_k\widehat{a}^\dagger)}{\text{Tr}(\widehat{a}\widehat{a}^\dagger)}. \quad (34)$$

If the scattering plane is the  $xy$  plane and the  $y$  axis points in the direction  $\mathbf{q} \times \mathbf{q}'$ , then due to parity conservation  $A_x = A_z = 0$  and the only non-zero component is  $A_y$ .

The deuteron vector and tensor analyzing powers are defined as

$$A_k = \frac{\text{Tr}(\widehat{a}\mathcal{P}_k\widehat{a}^\dagger)}{\text{Tr}(\widehat{a}\widehat{a}^\dagger)}, \quad A_{jk} = \frac{\text{Tr}(\widehat{a}\mathcal{P}_{jk}\widehat{a}^\dagger)}{\text{Tr}(\widehat{a}\widehat{a}^\dagger)}. \quad (35)$$

Parity conservation puts  $A_x, A_z, A_{xy}$  and  $A_{yz}$  to zero. So the non-vanishing and independent analyzing powers are defined by

$$iT_{11} = \frac{\sqrt{3}}{2}A_y, \quad T_{20} = \frac{1}{\sqrt{2}}A_{zz}, \quad T_{21} = -\frac{1}{\sqrt{3}}A_{xz}, \quad T_{22} = \frac{1}{2\sqrt{3}}(A_{xx} - A_{yy}). \quad (36)$$

Also spin transfer coefficients are given in the review. They have the same structure as the quantities above, with slightly different matrices to be inserted between  $\widehat{a}$  and  $\widehat{a}^\dagger$ .

### 3. Results

Our results for the differential cross section and nucleon analyzing power  $A_y$  (Fig. 1), deuteron vector  $iT_{11}$  and tensor analyzing  $T_{20}$  powers (Fig. 2), and  $T_{21}$  and  $T_{22}$  (Fig. 3) for nd elastic scattering at 3 MeV, using the AV14 NN potential, are shown together with the benchmark calculations of Kievsky et al. [24].

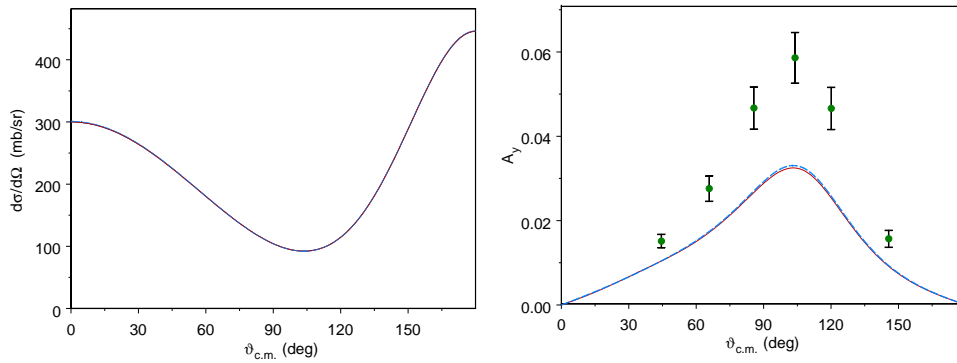


Fig. 1. Differential cross section and neutron analyzing power  $A_y$  for nd elastic scattering at 3 MeV lab energy as function of the c.m. scattering angle. The solid lines correspond to our results obtained with AV14 NN potential. The dashed lines correspond to results of Kievsky et al. obtained with the same NN potential [24]. The experimental data are from Ref. [25].

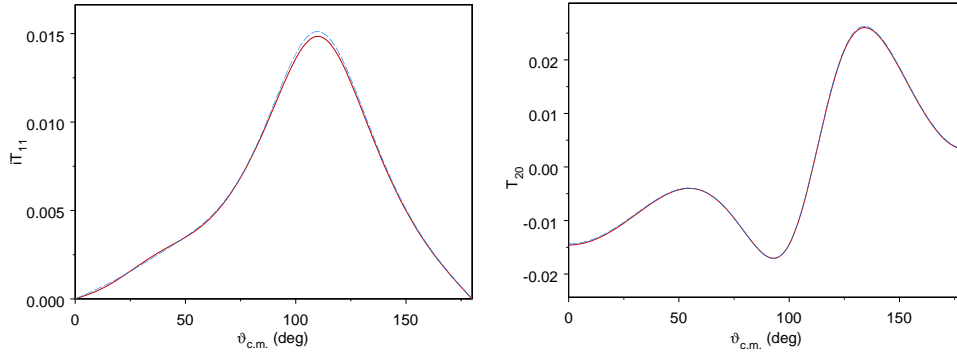


Fig. 2. Deuteron vector  $iT_{11}$  and tensor  $T_{20}$  analyzing power for  $nd$  elastic scattering at 3 MeV lab energy as function of the c.m. scattering angle. The notations are the same as in Fig. 1.

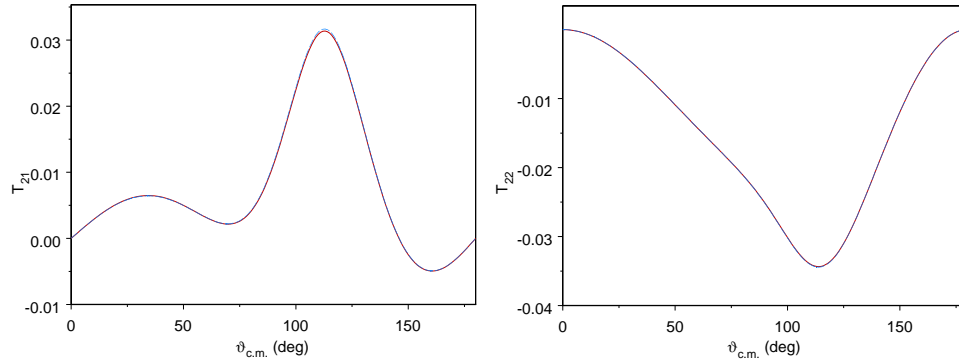


Fig. 3. Deuteron tensor analyzing powers  $T_{21}$  and  $T_{22}$  for  $nd$  elastic scattering at 3 MeV lab energy as function of the c.m. scattering angle. The notations are the same as in Fig. 1.

The theoretical predictions are compared with the experimental  $nd$   $A_y$  data at 3 MeV [26]. In both calculations all values of the total three-body angular momentum up to  $M = 15/2$  have been used. In our calculations, the total angular momentum of the pair of nucleons  $j_{23}$  has been taken up to 3, while in Ref. [24], this value was taken up to  $j_{23} = 4$ . It should be noted that in the case of  $nd$  scattering, increasing  $j_{23}$  by unity raises the number of partial waves from 62 up to 98. This difference presumably explains minor differences between these two calculations around the maximum values of  $A_y$  (Fig. 2) and of  $iT_{11}$  (Fig. 3), where the predictions of Kievsky et al. [24] are consistently higher by about 2–3%. Differences in  $T_{20}$ ,  $T_{21}$  and  $T_{22}$  are even smaller, about 1%.

For the  $pd$  elastic scattering at 3 MeV, results of our calculations for the differential cross section and proton analyzing power  $A_y$  are shown in Fig. 4 together

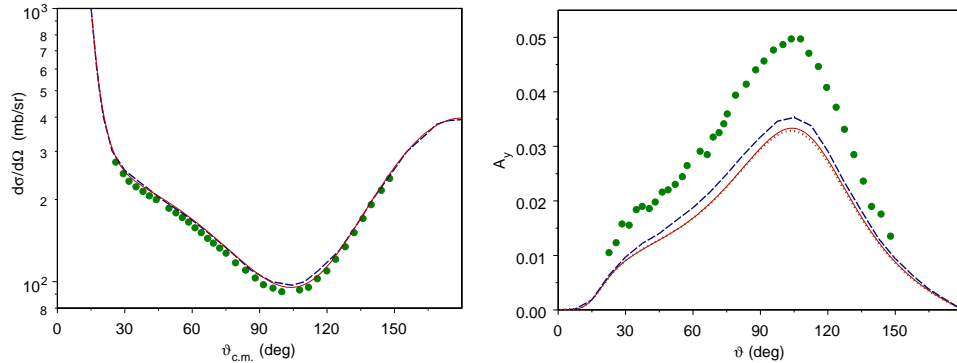


Fig. 4. Differential cross section and proton analyzing power  $A_y$  for pd elastic scattering at 3 MeV lab energy as function of the c.m. scattering angle. The solid lines correspond to our results obtained with AV14 NN potential. The dashed lines correspond to Deltuva et al. results [27] obtained with AV18 NN potential. The experimental data are from Ref. [28].

with those from the benchmark calculations of Deltuva et al. [27]. Our calculations have been performed using the AV14 NN potential and involving the correct asymptotic condition to take into account the Coulomb interaction while those of Ref. [27] used the AV18 NN potential and the screening and normalization procedure for the Coulomb force. All theoretical calculations are compared with the experimental data of Ref. [28]. All values of the total three-body angular momentum up to  $M = 15/2$  are used in our calculation, while in Ref. [27] value of  $M$  is much larger. We chose values of  $j_{23}$  up to 4 (up to 152 partial waves taken into account), whereas in Ref. [27] these values up to 5 have been used for the strong interaction (207 partial waves were taken into account). Again this truncation results in a small disagreement between our predictions for polarization observables and those from Ref. [27]. The results of calculations for the deuteron vector  $iT_{11}$  and tensor  $T_{20}$  analyzing powers as well as the experimental data [28] are shown in Fig. 5. The results of calculations for the deuteron tensor  $T_{21}$  and  $T_{22}$  analyzing powers as well as the experimental data [28] are shown in Fig. 6. Predictions of our calculations and those of Ref. [27] are in reasonable agreement.

In addition to our new results for nd and pd elastic scattering, we would like to present our new results for pd breakup scattering at  $E_{\text{lab}} = 14.1$  MeV obtained with the Malfiet-Tjon (MT) I-III potential. In our paper Ref. [22], results for inelasticities and phase shifts were obtained in  $s$ -wave approximation for both the strong and the Coulomb interactions. This means that only partial waves with  $l = 0$  were taken into account for nuclear and electromagnetic forces as it was explicitly pointed out and clearly explained in our paper. In Table 1 our old and new results together with those of Ref. [27] are given. Our new results presented in rows 2 – 6 were obtained for  $s$ -wave (MT)I-III potential and the Coulomb interaction was taken into account for different choices of sets of basis states (number of FNNM equations) depending on the maximum value of the two-body angular momentum  $j_{23}$ . In the

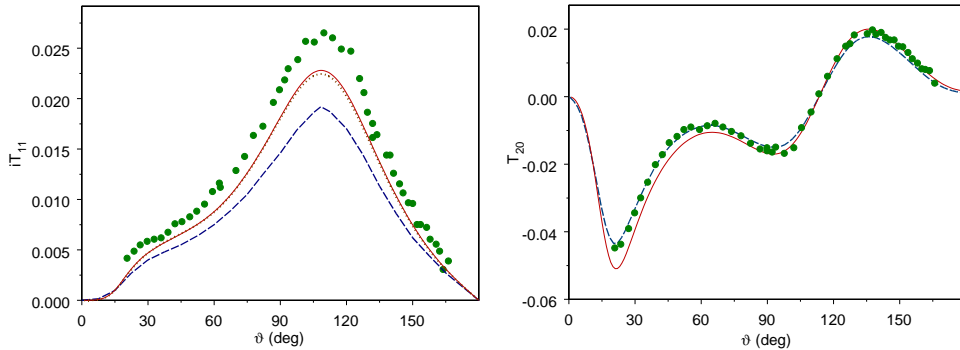


Fig. 5. Deuteron vector  $iT_{11}$  and tensor  $T_{20}$  analyzing power for  $pd$  elastic scattering at 3 MeV lab energy as function of the c.m. scattering angle. The notations are the same as in Fig. 4.

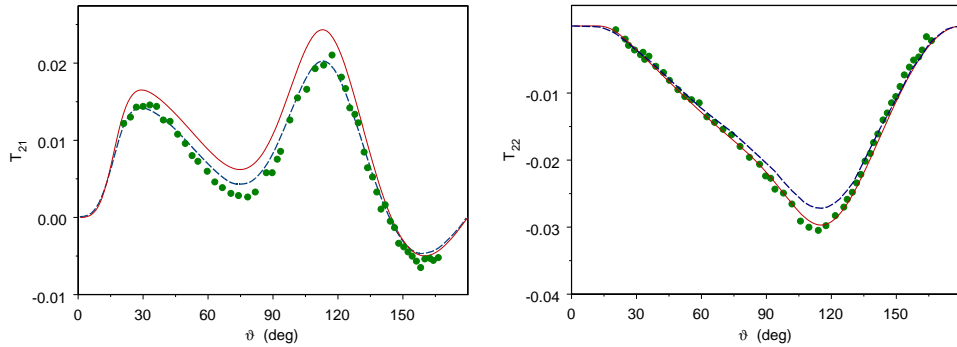


Fig. 6. Deuteron tensor analyzing powers  $T_{21}$  and  $T_{22}$  for  $pd$  elastic scattering at 3 MeV lab energy as function of the c.m. scattering angle. The notations are the same as in Fig. 4.

calculation, we have neglected the contribution of the basis states with the total isospin  $T = 3/2$  which makes the relative error less than 0.2%. In Table 1, one can see convergence of our results to those from Ref. [27]. Disagreement between inelasticity parameters is about 1% and is about 0.1 degree for phase shifts. As is pointed out in Ref. [27], the authors used the perturbation method. Our calculations have been performed by direct solution of the FNNM equations reduced to a set of linear equations with the resulting matrix having tri-block-diagonal structure. Small disagreements between results for  $s$ -wave  $pd$  breakup scattering can be explained by different numbers of partial waves taken into account (up to 126 in our calculations and up to 398 in calculations of Deltuva et al.). The authors in Ref. [27] have emphasized that for such large set of basis states direct solution is impossible and one has to apply the perturbation theory. Therefore, opposite to the claim of Ref. [27], when one compares results of calculations performed with almost the same input, our new result and those of Deltuva et al. agree very well.

TABLE 1. *pd* doublet (quartet) inelasticity  ${}^2\eta$  ( ${}^4\eta$ ) and phase shift  ${}^2\delta$  ( ${}^4\delta$ ) (in deg.) at  $E_{lab}=14.1$  MeV.  $\max j_{23}$  is maximal value of total angular momentum of pair (23) taken into account.  $N_{st}$  is the total number of Coulomb partial waves in the case  $T=1/2$ . For strong interaction only one partial wave ( $l=0$ ) is taken into account. The results from Ref. [22] obtained with a single Coulomb partial wave ( $l=0$ ) are given in the first row. Our results are given in rows numbered from 2 to 6. The result obtained in Ref. [27] using perturbation method is given in the last row.

	$\max j_{23}$	$N_{st}$	${}^2\eta$	${}^2\delta$	$N_{st}$	${}^4\eta$	${}^4\delta$
1	1	1	0.4929	108.06	1	0.9202	73.64
2	1	5	0.4827	108.14	14	0.9425	73.099
3	3	26	0.4899	108.47	46	0.9680	72.725
4	4	34	0.4906	108.465	62	0.9685	72.661
5	5	42	0.4904	108.48	78	0.9686	72.689
6	7	58	0.4906	108.48	100	0.9680	72.683
7	25	202	0.4984	108.44	398	0.9795	72.604

#### 4. Discussion

Our results for *nd* elastic scattering at 3 MeV and those from the KVP and momentum-space calculations are in very good agreement, and minor differences can be related to smaller values of  $j_{23}$  taken into account in our calculation. In the energy region from 1.2 to 10 MeV [29], theoretical predictions are 25–30% lower than the experimental data.

For *pd* elastic scattering excellent agreement within 1% between momentum-space and coordinate-space calculations based on a variational solution using a correlated hyperspherical expansion predictions at 3, 10 and 65 MeV incident nucleon energies have been demonstrated in Ref. [27]. Predictions of our calculation and that of Deltuva et al. [27] differ in the use of the NN potential and in values of the total three-body angular momenta  $M$  and of the total angular momenta of the pair of nucleons  $j_{23}$  taken into account. Our prediction is about 5% lower for  $A_y$  than that of Ref. [27], and surprisingly about 10% higher for  $iT_{11}$ . Predictions for tensor analyzing powers agree to better than 5%. Comparison with the experimental data of Ref. [28] confirms the  $A_y$  and  $iT_{11}$  puzzles. Both our calculations and those of Ref. [27] are lower than measured values of Ref. [28]. Results using the AV18 NN potential give better agreement with experimental data for  $T_{20}$  and  $T_{21}$ . However, surprisingly our calculation using the AV14 is in better agreement with the analyzing power  $T_{22}$ , possibly indicating differences between AV14 and AV18 potentials.

To end the discussion, we would like to compare our results for polarization

observables with those from Ref. [18]. In that paper, the authors have performed a detailed comparative study of modern three-nucleon models together in conjunction with the AV18 NN potential to calculate observables for pd elastic scattering at  $E_{\text{lab}} = 3$  MeV. The authors have shown that only the N<sup>2</sup>LOL TNF model allows to improve the description of  $A_y$  and  $iT_{11}$  noticeably. At the same time, the description of  $T_{21}$  becomes slightly worse and there is no change in  $T_{22}$ . In this regard we would like to note that our predictions obtained with the AV14 NN potential and without three-body forces coincide with the experimental  $T_{22}$  data [28] and are in good agreement with the result for  $iT_{11}$  from Ref. [18] obtained with three-body forces.

## 5. Conclusion

A very good agreement between predictions of our calculations and those of benchmark calculations demonstrates the soundness of our novel method providing thereby a new approach for calculating three-nucleon scattering including nucleon-nucleon and electromagnetic interactions. Our approach can and will be used to include three-nucleon forces and to perform additional studies using Kukulin's potential [30] and LS modified three-nucleon forces of Kievsky [31], particularly to study the  $A_y$  puzzle. It is well known that Nd polarization observables are the magnifying glass for studying  ${}^3P_J$  forces and calculations that rigorously include nuclear and electromagnetic interactions are very valuable.

Notwithstanding the significance of 3NF, our primary goal is to extend our study using AV14 NN potential and including the Coulomb potential to energies above the two-body threshold and to focus on breakup data and on established discrepancies. Our next step is to use the AV18 NN potential. As discussed in this article, we have already established interesting differences in  $T_{20}$ ,  $T_{21}$  and  $T_{22}$  most likely due to difference between the AV14 and AV18 NN potentials.

### Acknowledgements

We are very grateful to Prof. H. Witala for courteously giving the computer code to calculate nd observables. This work was supported by NSF CREST award HRD-0833184 and NASA award NNX09AV07A. The work of I. Š. was supported in part by the Croatian Ministry of Science.

### References

- [1] W. Glöckle, H. Witala, D. Hüber, H. Kamada and J. Golak, Phys. Rep. **274** (1996) 107.
- [2] E. O. Alt et al., Phys. Rev. C **17** (1978) 1981; A. Deltuva et al., Phys. Rev. C **72** (2005) 054004.
- [3] R. B. Wiringa et al., Phys. Rev. C **51** (1995) 38.
- [4] R. Machleidt et al., Phys. Rev. C **53** (1996) R1483.
- [5] V. G. J. Stocks et al., Phys. Rev. C **49** (1994) 2950.



- [6] R. B. Wiringa, R. A. Smith and T. L. Ainsworth, *Phys. Rev. C* **29** (1984) 1207.
- [7] S. A. Coon et al., *Nucl. Phys.* **317** (1979) 242; S. A. Coon and H. K. Han, *Few-Body Syst.* **30** (2001) 131.
- [8] B. S. Pudimer et al., *Phys. Rev. Lett.* **51** (1995) 4396; S. C. Pieper et al., *Phys. Rev. C* **64** (2001) 014001.
- [9] R. Machleidt, *Nucl. Phys. A* **790** (2007) 17 and references therein; U.-G. Meissner, *Nucl. Phys. A* **790** (2007) 129.
- [10] A. Deltuva et al., *Phys. Rev. C* **68** (2003) 024005; A. Deltuva et al., *Nucl. Phys. A* **790** (2007) 52.
- [11] P. Navratil, *Few-Body Syst.* **41** (2007) 117.
- [12] I. Šlaus, *Nucl. Phys. A* **790** (2007) 199.
- [13] W. Tornow et al., *Phys. Rev. Lett.* **49** (1982) 312; W. Gruebler et al., *Nucl. Phys. A* **398** (1983) 445; E. M. Neidel et al., *Phys. Lett. B* **552** (2003) 29, and references therein.
- [14] B. J. Wielinga et al., *Nucl. Phys. A* **261** (1976) 13; H. R. Setze et al., *Phys. Lett. B* **388** (1996) 229, and references therein; Z. Zhou et al., *Nucl. Phys. A* **684** (2001) 545; J. Ley et al., *Phys. Rev. C* **73** (2006) 064001.
- [15] C. R. Howel et al., submitted to *Phys. Rev. C*.
- [16] A. Kievsky et al., *Nucl. Phys. A* **577** (1994) 511; A. Kievsky et al., *Phys. Rev. C* **58** (1998) 3085; A. Kievsky et al., *Phys. Rev. C* **64** (2001) 024002; A. Kievsky et al., *Phys. Rev. C* **69** (2004) 014002.
- [17] E. O. Alt et al., *Nucl. Phys. B* **2** (1967) 167.
- [18] A. Kievsky, nucl-th ArXiv 1002.1254, Feb 5, 2010, and references therein; A. Kievsky, M. Viviani, L. Girlanda and L. E. Marcucci, *Phys. Rev. C* **64** (2010) 044003.
- [19] S. P. Merkuriev, C. Gignoux and A. Laverne, *Ann. Phys.* **99** (1976) 30.
- [20] A. A. Kvitsinsky, Yu. A. Kuperin, S. P. Merkuriev, A. K. Motovilov and S. L. Yakovlev, *Fiz. Elem. Chastits At. Yadra* **17** (1986) 267.
- [21] S. P. Merkuriev, *Ann. Phys. (N.Y.)* **130**, 3975 (1980);  
S. P. Merkuriev, *Acta Physica (Austriaca) Suppl.* **XXIII** (1081) 65.
- [22] V. M. Suslov and B. Vlahovic, *Phys. Rev. C* **69** (2004) 044003.
- [23] A. A. Kvitsinsky and C.-Y. Hu, *Few-Body Syst.* **12** (1992) 7.
- [24] A. Kievsky, M. Viviani, S. Rosati, D. Hüber, W. Glöckle, H. Kamada, H. Witala, and J. Golak, *Phys. Rev. C* **58** (1998) 3085.
- [25] J. E. McAninch, W. Haeberli, H. Witala, W. Glöckle and J. Golak, *Phys. Lett. B* **307** (1993) 13.
- [26] J. E. McAninch, L. O. Lamm and W. Haeberli, *Phys. Rev. C* **50** (1994) 589.
- [27] A. Deltuva, A. C. Fonseca, A. Kievsky, S. Rosati, P. U. Sauer and M. Viviani, *Phys. Rev. C* **71** (2005) 064003.
- [28] S. Shimizu, K. Sagara, H. Nakamura, K. Maeda, N. Nishimori, S. Ueno, T. Nakashima and S. Morinobu, *Phys. Rev. C* **52** (1995) 1193.
- [29] E. M. Neidel et al., *Phys. Lett. B* **552** (2003) 29.
- [30] V. I. Kukulín, 18th International IUPAP Conference on Few-Body Problems in Physics, FB18 - Book of Abstracts (2006) p.215.

[31] A. Kievsky, Phys. Rev. C **60** (1999) 031001.

### FADDEEV-LJEV RAČUN ELASTIČNOG RASPRŠENJA NUKLEON-DEUTERON ZA LAB ENERGIJU 3 MeV

Primijenili smo novu računalnu metodu za rješavanje problema nukleon-deuteron-skog raspršenja s raskidanjem radi proučavanja elastičnog raspršenja neutrona i protona na deuteronu primjenom Faddeev-Noyes-Noble-Merkurievih jednadžbi u običnom prostoru. Metoda se zasniva na "spline" razvoju po kutnoj varijabli i na poopćenju Numerove metode za hiperradijus. Poopćen je Merkuriev-Gignoux-Laverne-ov pristup za proizvoljne nukleon-nukleon potencijale i za proizvoljan broj parcijalnih valova. Za upadnu energiju nukleona od 3 MeV izračunali smo mjerne veličine nukleon-deuteron-skog raspršenja rabeći nabojno neovisan nukleon-nukleonski potencijal AV14, uključujući Coulombovu silu za raspršenje proton-deuteron. Ishodi računa se uspoređuju s ishodima drugih autora i s mjernih podacima za proton-deuteron raspršenje.